Short-term kinetics of rRNA degradation in Escherichia coli upon starvation for carbon, amino acid, or phosphate

Fessler, Mathias; Gummesson, Bertil; Charbon, Godefroid; Svenningsen, Sine Lo; Sørensen, Michael Askvad

Published in:
Molecular Microbiology

DOI:
10.1111/mmi.14462

Publication date:
2020

Document version
Early version, also known as pre-print

Short-term kinetics of rRNA degradation in *Escherichia coli* upon starvation for carbon, amino acid, or phosphate.

Mathias Fessler[1], Bertil Gummesson, Godefroid Charbon, Sine Lo Svenningsen* and Michael A. Sørensen*

Department of Biology, University of Copenhagen

Ole Maaløes Vej 5, 2200 Copenhagen N, Denmark

1) Present address: DTU Environment, Technical University of Denmark,

2800 Kongens Lyngby, Denmark

* Corresponding authors: Sine Lo Svenningsen, e-mail: SLS@bio.ku.dk Phone: +45 35322033 and Michael A. Sørensen, e-mail: MAS@bio.ku.dk Phone: +45 35323711

Running title: Kinetics of rRNA degradation in *E. coli*.

SUMMARY

Ribosomes are absolutely essential for growth but are, on the other hand, energetically costly to produce. Therefore, it is important to adjust the cellular ribosome levels according to the environmental conditions in order to obtain the highest possible growth rate while avoiding energy wastage on excess ribosome biosynthesis. Here we show, by three different methods, that the ribosomal RNA content of *Escherichia coli* is downregulated within minutes of the removal of an essential nutrient from the growth medium, or after transcription initiation is inhibited. The kinetics of the ribosomal RNA reduction vary depending on which nutrient the cells are starved for. The number of ribosomes per OD unit of cells is roughly halved after 80 minutes of starvation for isoleucine or phosphate, whilst the ribosome reduction is less extensive when the cells are starved for glucose. Collectively, the results presented here support the simple model proposed previously, which identifies inactive ribosomal subunits as the substrates for degradation, since the most substantial rRNA degradation is observed under the starvation conditions that most directly affect protein synthesis.

Keywords: *Escherichia coli*; stable RNA degradation; bacterial stress response; nutrient starvation; ribosomal RNA

INTRODUCTION

The molecular basis for the growth physiology of *Enterobacteria*, mainly *Escherichia coli*, has been studied for more than half a century. Early on it became evident that the growth kinetics of bacterial cultures are tightly linked to the regulation of bacterial ribosome content (see e.g. (Schaechter et al., 1958; Maaløe, 1979)). Since this fact was acknowledged, regulation of expression of the ribosomal components and the entire translational apparatus was studied intensively (see e. g. (Jinks-Robertson et al., 1983; Davis et al., 1986) (Paul et al., 2004) (Bremer & Dennis, 2008)). A main conclusion resulting from such studies is that transcription of the ribosomal RNA (rRNA) operons is the pivotal regulatory point that controls ribosome content, because ribosomal protein (r-protein) content is adjusted to nascent rRNA availability. This adjustment occurs via feedback mechanisms rooted in competition between binding sites for some of the ribosomal proteins on the rRNA and regulatory binding sites for the ribosomal proteins on the mRNA encoding them (Keener & Nomura, 1996). Furthermore, since rRNA was found to be stable during growth (e.g. (Gausing, 1977)), degradation of ribosomal components is considered a negligible factor in the control of cellular ribosome content. The genes encoding the three rRNAs; 5S, 16S, and 23S, are present in seven operons controlled by conserved, strong promoters with special features. The most important player in the transcriptional regulation of rRNA synthesis, and thereby growth rate, is the small molecule guanosine pentaphosphate or tetraphosphate (collectively herein (p)ppGpp) (Potrykus et al., 2011). Together with the protein DksA, (p)ppGpp binds to RNA polymerase, which affects promoter selectivity and reduces the rRNA promoter firing rates (Gummesson et al., 2013; Ross et al., 2016). In accordance with this role, there is an inverse correlation between the medium-dependent growth rate and the cellular content of (p)ppGpp during balanced growth (Lazzarini et al., 1971).

The established way to obtain reproducible results in bacterial growth physiology is to perform experiments on cultures in balanced exponential growth (Ingraham et al., 1983; Fishov et al., 1995),

and the vast majority of studies on ribosome content have been carried out under these conditions. Since both rRNA and transfer RNA (tRNA) are stable during exponential growth (Neidhardt, 1964; Gausing, 1977; Piir et al., 2011), the term stable RNA has been adopted for these cellular components over the years.

In contrast to balanced growth, rRNA is degraded after prolonged starvation for various essential metabolites ((Mandelstam & Halvorson, 1960; Ben-Hamida & Schlessinger, 1966; Jacobson & Gillespie, 1968a)). Ribosome degradation under starvation conditions can serve to enhance survival by making the released ribosomal building blocks available for other biosynthetic reactions. In addition to this role, the very reduction in the number of active ribosomes can allow the remaining ribosomes to maintain a functional translation elongation rate despite low substrate levels, as shown for *E. coli* growing at very slow rates in minimal medium supplemented with poor carbon and nitrogen sources (Dai et al., 2016). Similarly, during conditions of Mg^{2+} limitation, a stark reduction in the number of ribosomes frees up cytosolic Mg^{2+} which supports the Mg^{2+}-assisted assembly and functionality of the remaining ribosomes, thereby allowing protein synthesis to proceed (Pontes et al., 2016). It is thus clear that up- and down-regulation of ribosome content is central to both the growth and stress survival of bacterial cells.

In a previous study, we used a spike-in normalization strategy to show that tRNAs become unstable at the onset of amino acid starvation (Svenningsen et al., 2017), a situation comparable to a nutritional downshift or entry into stationary phase. Here we apply similar methodology to show that rRNA levels are also quickly downregulated by degradation upon starvation, and we back up our findings by rRNA quantification with fluorescence *in situ* hybridization and by quantification of acid-soluble RNA degradation products. Further, we show that the rate and extent of rRNA degradation depends on which macronutrient the cells are starved for. Our findings imply that during nutritional downshifts and other growth conditions that reduce protein synthesis activity, rRNA degradation

rates may be as important as rRNA synthesis rates for achieving the optimal number of ribosomes at the new growth condition.

RESULTS

Macromolecular changes upon valine-induced isoleucine limitation

We sought to measure rRNA degradation at the onset of amino acid starvation. To induce amino acid starvation in *E. coli* K-12 strains, it is common (e.g. (Laffler & Gallant, 1974; Traxler et al., 2008)) to take advantage of a metabolic anomaly in these strains, which is caused by a frameshift mutation in *ilvGM* that inactivates one of three isozymes common to the valine and isoleucine biosynthetic pathways. Since the other two isozymes, *ilvBN* and *ilvIH,* are subject to feedback inhibition by valine (R. I. Leavitt & Umbarger, 1961), the consequence of the frameshift mutation is that high valine concentrations inhibit not only valine biosynthesis, but also isoleucine biosynthesis (Richard I. Leavitt & Umbarger, 1962). Thus, addition of valine to *E.coli* K-12 cultures grown in isoleucine-free medium will result in isoleucine limitation.

We first quantified how severely valine addition affected the growth and macromolecular composition of our *E. coli* strain. Isoleucine starvation was induced by the addition of excess L-valine (400μg/ml) to balanced cultures of an *E. coli* strain auxotroph for pyrimidines and arginine, grown in a MOPS-buffered minimal glucose medium supplemented with uracil and arginine. By adding [^{14}C]-uracil and [^{3}H]-arginine we could monitor the accumulation of radioactivity in DNA, RNA and protein prior to and during isoleucine starvation (Fig. 1). Consistent with previous reports (G. N. Cohen, 1958; Temple et al., 1965), valine addition resulted in a reduced but nonzero growth rate, as measured by the optical density of the culture (Fig. 1A). We observed an immediate halt in the net protein synthesis upon valine addition (Fig. 1B), as well as a slight, but reproducible, reduction in the accumulation of ^{14}C into RNA, indicative of net RNA degradation (Fig. 1C). After a

transition period of approximately 80 minutes, the radioactivity incorporated into RNA and protein began to increase at a new constant rate similar to that of the other measured parameters, indicating *de novo* RNA and protein synthesis, and bacterial growth. The adverse effects of valine addition were less notable with regards to DNA synthesis (Fig. 1D) and counts of viable cells (Fig. 1E), which is in line with our expectations since *E. coli* is known to complete ongoing chromosomal replication events and reduce cell size upon amino acid starvation (Schreiber et al., 1995; Ferullo & Lovett, 2008; Maciag-Dorszynska et al., 2013). We have not been able to find an explanation for the continuation of macromolecular synthesis and growth in the presence of valine after the transition period, but remark that the identical result was obtained regardless of whether we only used a single dose of valine to initiate isoleucine starvation or supplemented the culture with additional valine every hour for the duration of the starvation period. This observation shows that the resumption of growth after the transition period is not due to a reduction in the extracellular valine concentration over time. Based on these measurements, we focused our study of rRNA degradation kinetics upon isoleucine starvation to the 80 minute transition period where no net synthesis of RNA or protein was observed.

Rapid turnover of ribosomal RNA upon amino acid starvation

To determine the changes in rRNA levels during amino acid starvation, we quantified the amounts of full-length 5S, 16S, and 23S rRNA species by northern blot, using spike-in cells for normalization, as described previously (Svenningsen et al., 2017). Briefly, an unstarved culture of spike-in cells, which are induced to express excessive amounts of the rarely used tRNA for selenocysteine ($tRNA^{Sec}$) upon addition of IPTG, was grown in parallel with the valine-treated wildtype culture, and harvested after IPTG induction. Prior to purification of RNA, defined volumes of the spike-in culture were mixed with each wildtype sample based on the OD units of the wildtype culture. This procedure allowed us

to quantify rRNA/OD by using the $tRNA^{Sec}$ band intensity in each lane of the northern blot as an internal standard. The use of spike-in cells allowed us to compare rRNA levels before and after starvation without making any assumptions about the levels of total RNA or any reference RNAs in the experimental samples.

A typical northern blot is shown in Fig. 2A. The rRNA levels are plotted relative to the average of three samples harvested during balanced growth before the addition of valine. After only 10 minutes of starvation, the levels of rRNA drop to ~85% of the pre-starvation levels, and after 80 minutes rRNA levels have decreased to 55% for 16S and 23S RNAs, and to 75% for the 5S RNA (Fig. 2B). Note that rRNA from the spike-in cells did not contribute significantly to the 16S and 23S band intensities (Fig. 2A, lane 14). At the 80 min timepoint, the culture was replenished with isoleucine, leading to immediate resumption of rRNA synthesis (Fig. 2B) and growth soon resumed at the pre-starvation rate (Fig. 2C).

Different types of starvation and stress result in different degrees of rRNA reduction.

It is well established that rRNA eventually becomes unstable when bacteria are deprived of a carbon source (Jacobson & Gillespie, 1968b; Zundel et al., 2009), and extensive RNA degradation has also been reported for starvation for other nutrients, such as nitrogen (Ben-Hamida & Schlessinger, 1966; R. Kaplan & Apirion, 1975) and phosphate (Maruyama & Mizuno, 1970). However, it is not clear to what extent the kinetics rRNA reduction differ between different types of starvation (Deutscher, 2003). We first focused on glucose starvation, which was the type of starvation employed when the rRNA degradation pathway was determined (Sulthana et al., 2016). Despite the differences in metabolic function, glucose starvation and amino acid starvation provoke some of the same cellular responses. Both amino acid and glucose starvation eventually lead to stabilization of the stress

response sigma factor RpoS (Traxler et al. 2008, Mandel and Silhavy 2004) and, thus, activation of the general stress response. For this reason, the two stress conditions might be expected to have comparable impacts on rRNA levels. To starve for glucose, exponentially growing cells were filtered and resuspended in minimal medium lacking glucose. As shown in Fig. 3A, glucose starvation lead to a reduced rRNA content, but the rate of reduction in rRNA levels was much slower than under amino acid limitation. Specifically, 80 minutes of glucose starvation lead to a 10% reduction of the 16S and 23S RNAs (Fig 3A).

Next, we starved the cells for phosphate to assess how rRNA levels are affected when the supply of an essential component of the RNA-backbone is removed. To do this, cultures in balanced growth were filtered and resuspended in medium without phosphate. This type of starvation led to the most severe rRNA reduction observed, amounting to a 60% reduction over 80 minutes for rRNA of the two large subunits (Fig 3B). Finally, to further investigate how protein synthesis activity affects rRNA instability we inhibited RNA synthesis with rifampicin, which binds RNA polymerase and inhibits transcription initiation (Campbell et al., 2001). Ribosomes are affected by rifampicin in two ways. First, transcription of rRNA is blocked and second, the demand for translational activity is diminished as transcription of mRNA is inhibited as well. To assess the rRNA degradation upon rifampicin exposure, rifampicin was added to cultures in balanced growth, and samples harvested before and up to 80 minutes after rifampicin addition were treated as above. It was not possible to measure optical density after addition of rifampicin, since rifampicin affects the absorbance of light at the relevant wavelengths. Therefore, normalization was done under the assumption that the OD_{436} of the culture did not change after rifampicin addition. Fig. 3C shows that all three rRNAs were degraded rapidly in response to rifampicin. Within the first 10 minutes, the amounts of 16S and 23S rRNA had been reduced to approximately 50% of the level found during balanced growth. After the

initial rapid drop, rRNA levels stabilized for the remainder of the experiment. Thus, for both amino acid starvation and rifampicin treatment, the amount of rRNA is roughly halved at the end of the experiment. However, the kinetics are different, as the majority of the full-length rRNA disappears within the first 10 minutes in rifampicin-treated cells, whereas the isoleucine-limited cells lose their rRNA at a slower rate for an extended time.

E. coli RNA degradation *in situ*

To validate the rRNA levels observed in the Northern blots, we conducted a series of fluorescent *in situ* hybridization (FISH) experiments. FISH is a powerful alternative method for evaluating rRNA breakdown because no purification steps are required. Instead of purifying the RNA, the relative rRNA levels inside single cells are measured. There is a direct correlation between the cellular rRNA content of cultures growing at different rates, and the intensity of the fluorescent signal from an rRNA-targeted oligonucleotide probe, meaning that the method allows for rRNA quantitation (DeLong et al., 1989). This method excludes any artifacts of the RNA extraction process that in theory could affect growing and starving cells differently, like differences in cell size (compare light scatter in Fig. 4A and 4B). Cells harvested from balanced growth and following 80 minutes of isoleucine limitation, glucose starvation, phosphate starvation or rifampicin treatment were fixed in formaldehyde. After cell permeabilization, a fluorescent probe recognizing a sequence in the 3‘-end of the 16S subunit was allowed to hybridize overnight, excess probe was washed away, and the fluorescence intensity was measured by flow cytometry. The relative 16S fluorescence is shown in Fig. 4. The measured fluorescence values of individual cells have been divided by the cell size measurement to more accurately reflect the rRNA concentration.

The results from the FISH experiments strongly agree with the northern blot data, confirming that rRNA is indeed degraded extensively during short-term starvation for all the tested nutrients. In both northern and FISH experiments, phosphate starvation causes the most drastic drop in rRNA levels, followed by isoleucine starvation, and finally glucose starvation, which has the smallest short-term impact on rRNA stability. In the case of rifampicin treatment, the results of the FISH experiment did only qualitatively agree with the other experiments, since the FISH quantification only indicates approximately 20% degradation of 16S rRNA after 80 min.

To compare the FISH data with our northern blots, we used a northern probe with the exact same sequence as the FISH probe and the results were the same under all four stress conditions (Suppl. Fig. S1).

Finally, we verified that the FISH probe bind to cellular RNA, as no fluorescent signal was observed in cells treated with RNase A after fixation, regardless of whether the cells had been subject to isoleucine limitation (Fig. 5C).

The pool of RNA degradation products increases during carbon-, amino acid-, and phosphate-starvation as well as rifampicin treatment

To further validate the fast disappearance of rRNA during starvation, a different approach based on the differential precipitation of short oligonucleotides and longer RNA molecules in acid (L. Cohen & Kaplan, 1977), was adapted. In short, bacterial cultures prelabelled with [^{14}C]-uracil were filtered into medium containing rifampicin, starvation media, or control medium allowing continued exponential growth. At each sampling point, two aliquots of the same culture were harvested into 5% TCA and 4M formic acid, respectively. The ^{14}C found in the TCA precipitable material is a measure of pyrimidines found in RNA and DNA polymers longer than ~16 nt (Cleaver & Boyer, 1972), while counts found in the supernatant of the formic-acid treated cells represents mononucleotides and short

oligonucleotides because the formic acid treatment permits these short mono-, di- and oligomers to leak out of the cells (L. Cohen & Kaplan, 1977).

Since rRNA accounts for approximately 85% of total cellular RNA in exponential growth (Maaløe, 1979; Bremer & Dennis, 1996), and because rRNA (and tRNA) stability greatly exceeds mRNA stability during growth, the majority of the [^{14}C]-uracil would be incorporated into rRNA at the time the cells were exposed to rifampicin or nutrient starvation. Therefore, an increase in the free mono- and oligonucleotides primarily reflect nucleotides or short fragments released from ribosomes, and to a lesser extent possibly tRNA. This method was used previously to demonstrate degradation of rRNA during glucose starvation (Zundel et al., 2009). Our experiment confirmed the reported accumulation of ^{14}C in the formic-acid-soluble fraction upon glucose starvation. In our measurements, the percentage of formic-acid-soluble radioactivity increased steadily until reaching a plateau at ~7% after 2.5 hours of glucose starvation (Fig. 5, triangles). Very similar results were obtained after isoleucine limitation (Fig. 5, squares). By contrast, a plateau was not reached for the duration of the phosphate starvation experiment, and the amount of formic-acid-soluble ^{14}C-labeled material was much higher, reaching 28% after 3 hours of starvation. Similarly, formic-acid-soluble counts from cells treated with rifampicin did not reach a plateau, instead the acid-soluble fraction increased at an almost constant rate over the three-hour period, reaching 14%. In comparison, acid-soluble counts from the exponentially growing control culture stayed at a basal level very close to 0% for the duration of the experiment. Replenishing the missing nutrient restored growth and lead to a rapid decrease in the acid-soluble fraction in all cases (isoleucine, glucose or phosphate addition to the starved cells), in accordance with resumed net RNA synthesis.

As the formic acid ^{14}C-release assay reports on the free mono- and oligo-nucleotides and derivatives, a pool whose size depends on RNA degradation but also on the rates of reuse of the nucleotides or

their constituents for other metabolic reactions, it cannot be used to determine the kinetics of rRNA degradation directly. Nevertheless, the increase of the free nucleotide pool strongly supports the observed induction of rRNA degradation shown in Figs. 2-5 upon nutrient starvation or rifampicin treatment.

DISCUSSION

With the present set of experiments, we show that the levels of *E. coli* rRNA are dynamically regulated upon nutrient downshifts and starvation, and that regulation of rRNA levels does not only occur at the level of rRNA promoter activity but must also occur by degradation of existing rRNA in response to different types of starvation. rRNA breakdown has been reported before (Ben-Hamida & Schlessinger, 1966) but often under aberrant conditions (Okamura et al., 1973) (Ruth Kaplan & Apirion, 1974; R. Kaplan & Apirion, 1975) or with only a few time-points in studies that were focused on the mechanism, rather than the kinetics of rRNA degradation (Zundel et al., 2009; Basturea et al., 2011; Sulthana et al., 2016). Here, we used a method relying on the addition of spike-in cells expressing high amounts of a reference RNA to accurately quantify bacterial RNA content. The advantage of the spike-in method is that it allows for normalization of sample signals, which is required to reduce noise caused by variations in RNA recovery and blotting, without making assumptions about the existence of an invariable endogenous reference RNA or invariable total RNA contents of the cells, before and after starvation (Stenum et al., 2017; Svenningsen et al., 2017; Sorensen et al., 2018). Since recovery of RNA from starved cells could be reduced compared to growing cells due to physiological changes of the cell envelope and size of the cells, we also performed FISH experiments (Fig. 5) and formic acid solubility experiments (Fig. 6), which do not involve RNA purification, to rule out that variations in RNA recovery could have biased our results.

A key question is how degradation of rRNA is triggered. The Deutscher group has elegantly elucidated the molecular degradation pathway of rRNA in cells starved for glucose (Zundel et al., 2009; Sulthana et al., 2016) and shown that the initial points of ribonuclease cleavage of the rRNA occur at the interface of the 30S and 50S subunits, suggesting that rRNA is primarily degraded when the two subunits are apart. These findings lend strong support to a model proposed previously by the same group, in which ribosomal inactivity is the trigger for degradation (Deutscher, 2003). This appealingly simple model predicts a dynamic scenario where the cellular ribosome content is continually adjusted to the protein synthesis activity because the degradation machinery specifically eliminates unengaged ribosomes. The model is also supported by the finding that isotope-labelled tagged rRNAs were stable during exponential growth, and somewhat stable after establishment of the stationary phase, but quite unstable during the transition from exponential growth into stationary phase where the protein synthesis activity would be declining (Piir et al., 2011). M. Deutscher's model fits very well with our northern blot data which are summarized in Figure 6 for the case of 16S rRNA.

First, we found that glucose starvation caused the weakest and slowest reduction of rRNA compared to any of the other treatments (Fig. 6). Glucose starvation does not directly affect the translation process, and both substrate (aminoacylated tRNA) and template (mRNA) are expected to be present in relatively high amounts while the cells prepare for stationary phase survival utilizing the glycogen storage for energy supplies. Second, the translation process is directly affected by the downshift caused by valine addition, due to the lack of isoleucyl-tRNA substrate, and net protein synthesis was zero immediately after valine addition (Fig. 1). Consistent with reduced protein synthesis, our measurements reproducibly showed a net loss of RNA for the first 80 minutes after valine addition (Fig. 1). Indeed, during the same time span, northern blot analysis showed that rRNA levels were reduced to 50-60 % of their pre-starvation levels (Fig. 2). Our interpretation is that a fraction of the

316 ribosomes were available for degradation in the transition period until a new steady state was
317 reached, due to the lack of isoleucyl-tRNA substrate for translation. Lastly, the removal of phosphate
318 from the medium resulted in a faster and more extensive reduction in the rRNA content than the other
319 starvation types, and the only treatment that caused an even faster reduction of rRNA than phosphate
320 starvation was the addition of rifampicin (Fig. 3 and Fig. 6). Using rifampicin, transcription initiation
321 was prevented and since the average mRNA half-life is only a few minutes (Liang et al., 2000),
322 rifampicin causes a rapid decline in mRNA concentrations and therefore a fast decline in protein
323 synthesis (Pedersen et al., 1978), which would leave ribosomes inactive and available for
324 degradation. Similarly, by removal of all phosphate from the medium, RNA synthesis decreases to
325 low levels due to lack of substrate (St John & Goldberg, 1980), although cells have some residual
326 transcriptional activity due to the phosphate stored in poly-P_i (Rao et al., 1998) and presumably
327 recycle nucleotides from rRNA as well. Rapid degradation of rRNA during phosphate starvation, and
328 even faster degradation after rifampicin addition therefore fits very well with the inactivity model
329 coined by M. Deutscher's group.
330 We observed the greatest release of the radioactive label in the cells under phosphate starvation (Fig.
331 5). Up to 70% of total cellular phosphate is found in RNA during rapid growth, while the remainder
332 is mainly incorporated in the phospholipid membrane and to a lesser extent in DNA. Presumably, the
333 phosphate released from the breakdown of rRNA during phosphate starvation is recycled for use
334 elsewhere in the cells, so that the formic-acid-soluble [^{14}C] is mainly in the form of the [^{14}C]-uracil
335 nucleobase. Indeed, extra- and intracellular accumulation of the uracil nucleobase has been reported
336 at the entry to stationary phase (Rinas et al., 1995).
337 The ribosome content of *E. coli* growing balanced in chemostats on limiting carbon, nitrogen or
338 phosphate concentrations has been measured recently (Li et al., 2018) and it was confirmed that
339 ribosome content decreases with a decrease in the quality of the growth medium. Furthermore,

cultures growing at the same low rate but limited for glucose or nitrogen had equally low ribosome levels while, surprisingly, phosphate-limited cells growing at the same rate contained down to 50% fewer ribosomes (Li et al., 2018) This result indicates that phosphate starvation may cause very limited ribosome concentrations. The ribosome content of these steady-state growing chemostat cultures could have been reached solely by the ppGpp-mediated reduced synthesis rates of rRNA, compared to cultures growing in saturating levels of nutrients. Thus no role for rRNA degradation can be evoked for these chemostat experiments. By contrast, we studied rRNA degradation in response to an abrupt change where the nutrient went from being in excess to exhaustion in a matter of seconds. The response to this abrupt change was a substantial drop in rRNA/OD both for amino-acid-starved and phosphate-starved cells, and a more modest drop for glucose-starved cells. The drop in rRNA levels cannot be explained solely by reduced rRNA synthesis and growth dilution in our experiments, but must also result from rRNA degradation, as is most clearly shown by an early net reduction of rRNA per culture volume (Fig. 1C , S2 & Supplementary Discussion) and the accumulation of RNA degradation products (Fig. 5). Based on the steady-state measurements made by Li et al. (Li et al., 2018) we assume that starvation beyond 80 min in our experiments would have eventually led to a situation where phosphate-starved cells had the lowest rRNA content while glucose- and amino-acid-starved cells would have reached similar rRNA levels at times where the stored glycogen had been exhausted in the glucose-starved cells.

To summarize, our results show that rRNA breakdown can be an important factor when bacteria adapt to new growth conditions where the optimal steady-state ribosome content is lower than before the shift. While these results unequivocally demonstrate that a fraction of rRNA is being degraded upon rifampicin treatment and the three types of starvation, the differences in the magnitude of the net loss of rRNA are proportional to the expected differences in rRNA synthesis rates under the four

conditions. Specifically, rRNA synthesis rates are initially limited only by the effect of ppGpp on transcription from the P1 promoter of rRNA operons in the cases of glucose-starvation and isoleucine-starvation (Maaløe, 1966; Sarmientos & Cashel, 1983), while rRNA synthesis would be inhibited both by ppGpp (Spira et al., 1995) and lack of nucleotide substrates in the case of phosphate starvation (St John & Goldberg, 1980), and rRNA synthesis would be completely eliminated shortly after rifampicin treatment (Pato & Von Meyenburg, 1970). Thus, the up-regulation of rRNA degradation upon the different treatments can be understood as an additional layer of regulation acting additively with the down-regulation of rRNA synthesis to rapidly adjust rRNA levels to the new condition. We have illustrated the interplay between rRNA synthesis and breakdown in Fig. 7. In this figure, the blue arrows show the well-described pathways for regulation of the production of translational RNA (rRNA and tRNA) where an improvement of the growth medium leads to a higher saturation of translating ribosomes, followed by a reduction of the ppGpp production and an increase in the transcription rate of translational RNA genes and an increase in the growth rate. However, less well recognized, and here illustrated by red arrows pointing to the RNA degradation function in Fig. 7, an abrupt nutrient downshift may lead to degradation of unengaged ribosomal subunits (Zundel et al., 2009; Sulthana et al., 2016), nascent rRNA uncovered by ribosomal proteins (Jain, 2018) and vacant tRNA (Svenningsen et al., 2017). RNA degradation probably happens to replenish important pools of building blocks for the cell to be able to reorganize expression patterns to cope with the nutritional down shift, but maybe also to establish balanced pools of translational RNA under circumstances where dilution by growth is either a very slow process or not an option at all, like at entrance into stationary phase.

In conclusion, we suggest that degradation of translational RNA upon starvation is an important regulatory phenomenon that help cells cope with stresses that decrease translational activity. Furthermore, this stress-related rRNA breakdown is not unique to *E. coli*. For example, the ribosomal

content of *Pseudomonas flourescens* strain Ag1 dropped to ~45% of the pre-starvation level after 2 hours of carbon starvation (Boye et al., 1995), and in the gram-positive bacterium *Lactococcus lactis*, rRNA levels dropped to 30% after 1 hour of sublethal heat treatment ($43°C$) (Hansen et al., 2001). Lastly, in their seminal paper from 1958 on *Salmonella* transitions between different physiological states by Kjeldgaard, Maaløe and Schaechter (Kjeldgaard et al., 1958), a net drop in RNA levels is also evident upon the downshift of a *Salmonella* culture from a defined complete medium to the same medium lacking amino acids.

Despite these examples, we think the labile nature of stable RNA under stress has generally been overlooked because the amount of total RNA harvested per cell is difficult to measure quantitatively, but this challenge is surmounted by the addition of spike-in cells for normalization of recovery during all steps of RNA purification.

EXPERIMENTAL PROCEDURES

Strains, media and growth conditions

Two derivatives of the *E. coli* K-12 MG1655 strain were used. For all experiments resulting in Northern blots, FISH experiments or RNA-seq the strain MAS1081 (MG1655 rph^+ $gatC^+$ $glpR^+$) was used. The cells were grown at 37°C in MOPS minimal medium (Neidhardt et al., 1974) supplemented with 0.2% glucose, and were grown for at least 10 generations in exponential phase before every experiment unless otherwise stated. Isoleucine starvation was induced by adding valine to a final concentration of 400 μg/ml (Leavitt and Umbarger, 1962), glucose and phosphate starvation was induced by filtering the cells, washing in medium without glucose or phosphate, and subsequently resuspending them in MOPS media lacking either glucose or phosphate. These

412 operations were performed at 37° C in less than two min. Rifampicin was added to a final
413 concentration of 100 μg/ml.
414 For the internal standard in the Northern blots MAS1074 (Svenningsen et al., 2017) a BL21(DE3) +
415 pET11a(*selC*) strain was used, which was also grown in MOPS media with 0.2% glucose at 37°C.
416 $tRNA^{SelC}$ expression was induced by adding IPTG to a final concentration of 1mM.
417 The DNA, RNA and protein synthesis experiments were done in a MAS1081 background made
418 auxothroph for pyrimidines and arginine by removing the *pyrE* and *argG* genes from the WT
419 background i.e. in MAS1083: rph^{+} $gatC^{+}$ $glpR^{+}$ *ΔpyrE::tet ΔargG::(cat sacB)*.
420

421 **RNA extraction, blotting, hybridization and quantification**

422 1.5 ml samples were harvested by transferring into 300 μl stop-solution consisting of 95% ethanol
423 and 5% phenol at 0°C. Samples were kept at 0°C until the final sample had been harvested. At this
424 point the spike-in cells were added to each WT sample (5% spike-in culture was added based on OD)
425 and subsequently total RNA was extracted with hot phenol. A detailed description of the northern
426 blot procedure is present in Supplementary methods.
427 Each membrane was probed for 5S rRNA, 16S rRNA, 23S rRNA and $tRNA^{Sec}$ (Sequences in Table
428 S1). Normalization was done by calculating the ratio between the counts of a given rRNA and
429 $tRNA^{Sec}$ in the same lane of the blot, and this value was then plotted relative to the three samples
430 harvested immediately before inducing starvation.
431

432 **Macromolecular synthesis measurements**

433 The MG1655 rph^{+} $gatC^{+}$ $glpR^{+}$ *ΔpyrE ΔargG* strain was grown overnight at 37°C in MOPS media
434 supplemented with 0.2% glucose, 20 μg/ml uracil and 80 μg/ml arginine. The next morning, once the
435 O/N culture reached OD_{436} = 0.1, 0.33 μCi/ml [^{3}H]-arginine (54.5 Ci/mmol) and 0.03 μCi/ml [^{14}C]-

uracil (58 mCi/mmol) was added to the culture. Every 20 minutes 0.5 ml samples were harvested into 5 ml 5% TCA and 0.5 ml 0,5 M NaOH both kept at 0°C. Further details for treatment of samples for measuring macromolecular synthesis and CFU determinations, see Supplementary methods.

Monitoring of rRNA degradation in vivo

MAS1081 (wt) cells were left to grow overnight in MOPS media with 0.2% glucose. The following day the culture was diluted 500x and 0.05 μCi /ml of [^{14}C]-uracil (58 mCi/mmol) was added to label total RNA in the cells. Incorporation of the labeled uracil was considered to be fast and finished generations before the actual experiment. After the 5 generations, the culture was filtered to induce starvation and remove any remaining unincorporated [^{14}C]-uracil from the medium. The cells were resuspended in media with rifampicin or media inducing either isoleucine starvation, glucose starvation, phosphate starvation or exponential growth. The release of radioactive degradation products were measured essentially as described by (Zundel et al., 2009) but see Supplementary methods for details.

Fluorescent in situ hybridization

4 samples of 1 ml were harvested from an overnight culture with WT cells immediately before inducing starvation (or adding rifampicin) and another 4 samples after 80 minutes of starvation. Samples were treated as described by Parsley et al. (2010). Fluorescence was measured with an Apogee A10 Bryte flow cytometer equipped with a mercury arc lamp. A G1 filter cube (520-560 nm for excitation and emission at > 590 nm) was used. Two parameters were measured in the flow cytometer – forward light scatter (measure of size) and fluorescence. For each sample the fluorescence/size ratio was calculated and the appropriate background was subtracted. The formula is

shown below, where "x" denotes the condition (exponential growth, isoleucine starvation, glucose starvation, phosphate starvation, rifampicin treatment or RNase treatment):

$$value_{sample(x)} = (fluorescence_{sample(x)}/size_{sample(x)}) - (fluorescence_{background(x)}/size_{background(x)})$$

Finally, the mean of the 4 starvation values was normalized to the mean of the 4 exponential phase values, which was set to 1.

Statistical testing

To test for significance a two-sided paired t-test was applied. The cut-off for significance was a p-value below 0.05. To use the t-test, the data must follow a normal distribution, which was tested for with a Shapiro-Wilk test. A p-value above 0.1 from this test suggests that the data is normally distributed.

Acknowledgements

The authors thank Marit Warrer for excellent technical assistance. Danish Council for Independent Research, Natural Sciences [1323-00343B to S.L.S.]; Novo Scholarship to M.F.; Danish National Research Foundation [DNRF120 to S.L.S. and M.A.S.]. Funding for open access charge: The Danish National Research Foundation. Conflict of interest statement. None declared.

Author contributions

M. F., S.L.S and M.A.S. wrote the manuscript. S.L.S., M.A.S. and M. F. designed experiments; M. F., B. G., G. C. and M.A.S. performed experiments; M.A.S. and S.L.S. conceived and designed research.

Graphical Abstract

Abbreviated Summary

Escherichia coli ribosomal RNA is highly unstable right after nutritional deprivation. The kinetics differ depending on the type of starvation, in a manner consistent with active degradation of the unengaged ribosomes.

REFERENCES

Basturea, G. N., Zundel, M. A., & Deutscher, M. P. (2011). Degradation of ribosomal RNA during starvation: comparison to quality control during steady-state growth and a role for RNase PH. *RNA, 17*(2), 338-345. doi:10.1261/rna.2448911

Ben-Hamida, F., & Schlessinger, D. (1966). Synthesis and breakdown of ribonucleic acid in Escherichia coli starving for nitrogen. *Biochim Biophys Acta, 119*(1), 183-191. Retrieved from https://www.ncbi.nlm.nih.gov/pubmed/5335523

Boye, M., Ahl, T., & Molin, S. (1995). Application of a strain-specific rRNA oligonucleotide probe targeting Pseudomonas fluorescens Ag1 in a mesocosm study of bacterial release into the environment. *Appl Environ Microbiol, 61*(4), 1384-1390. Retrieved from https://www.ncbi.nlm.nih.gov/pubmed/7538276

Bremer, H., & Dennis, P. (2008). Feedback control of ribosome function in Escherichia coli. *Biochimie, 90*(3), 493-499. doi:10.1016/j.biochi.2007.10.008

Bremer, H., & Dennis, P. P. (1996). Modulation of chemical composition and other parameters of the cell by growth rate. In F. C. Neidhardt (Ed.), *Escherichia coli and Salmonella: Cellular and molecular biology* (2nd ed.). Washington DC: ASM Press.

Campbell, E. A., Korzheva, N., Mustaev, A., Murakami, K., Nair, S., Goldfarb, A., & Darst, S. A. (2001). Structural Mechanism for Rifampicin Inhibition of Bacterial RNA Polymerase. *Cell, 104*(6), 901-912. doi:https://doi.org/10.1016/S0092-8674(01)00286-0

Cashel, M., & Gallant, J. (1969). Two compounds implicated in the function of the RC gene of *Escherichia coli*. *Nature (London), 221*, 838-841.

518 Cleaver, J. E., & Boyer, H. W. (1972). Solubility and dialysis limits of DNA oligonucleotides. *Biochimica*
519 *et Biophysica Acta (BBA) - Nucleic Acids and Protein Synthesis, 262*(2), 116-124.
520 doi:https://doi.org/10.1016/0005-2787(72)90224-9
521 Cohen, G. N. (1958). [Synthesis of abnormal proteins in E. coli K 12 cultured in presence of valine].
522 *Ann Inst Pasteur (Paris), 94*(1), 15-30.
523 Cohen, L., & Kaplan, R. (1977). Accumulation of nucleotides by starved Escherichia coli cells as a
524 probe for the involvement of ribonucleases in ribonucleic acid degradation. *J Bacteriol,*
525 *129*(2), 651-657. Retrieved from https://www.ncbi.nlm.nih.gov/pubmed/320188
526 Dai, X., Zhu, M., Warren, M., Balakrishnan, R., Patsalo, V., Okano, H., . . . Hwa, T. (2016). Reduction
527 of translating ribosomes enables Escherichia coli to maintain elongation rates during slow
528 growth. *Nature Microbiology, 2*, 16231. doi:10.1038/nmicrobiol.2016.231
529 https://www.nature.com/articles/nmicrobiol2016231#supplementary-information
530 Davis, B. D., Luger, S. M., & Tai, P. C. (1986). Role of ribosome degradation in the death of starved
531 Escherichia coli cells. *J Bacteriol, 166*(2), 439-445. Retrieved from
532 https://www.ncbi.nlm.nih.gov/pubmed/2422153
533 DeLong, E. F., Wickham, G. S., & Pace, N. R. (1989). Phylogenetic stains: ribosomal RNA-based probes
534 for the identification of single cells. *Science, 243*(4896), 1360-1363. Retrieved from
535 https://www.ncbi.nlm.nih.gov/pubmed/2466341
536 Deutscher, M. P. (2003). Degradation of stable RNA in bacteria. *J Biol Chem, 278*(46), 45041-45044.
537 doi:10.1074/jbc.R300031200
538 Dong, H. J., Nilsson, L., & Kurland, C. G. (1996). Co-variation of tRNA abundance and codon usage in
539 Escherichia coli at different growth rates. *Journal of Molecular Biology, 260*(5), 649-663.
540 doi:DOI 10.1006/jmbi.1996.0428
541 Ferullo, D. J., & Lovett, S. T. (2008). The stringent response and cell cycle arrest in Escherichia coli.
542 *PLoS genetics, 4*(12), e1000300-e1000300. doi:10.1371/journal.pgen.1000300
543 Fishov, I., Zaritsky, A., & Grover, N. B. (1995). On microbial states of growth. *Mol Microbiol, 15*(5),
544 789-794.
545 Gausing, K. (1977). Regulation of ribosome production in Escherichia coli: Synthesis and stability of
546 ribosomal RNA and of ribosomal protein messenger RNA at different growth rates. *Journal*
547 *of Molecular Biology, 115*(3), 335-354. doi:https://doi.org/10.1016/0022-2836(77)90158-9
548 Gummesson, B., Lovmar, M., & Nyström, T. (2013). A Proximal Promoter Element Required for
549 Positive Transcriptional Control by Guanosine Tetraphosphate and DksA Protein during the
550 Stringent Response. *Journal of Biological Chemistry, 288*(29), 21055-21064.
551 doi:10.1074/jbc.M113.479998
552 Hansen, M. C., Nielsen, A. K., Molin, S., Hammer, K., & Kilstrup, M. (2001). Changes in rRNA levels
553 during stress invalidates results from mRNA blotting: fluorescence in situ rRNA hybridization
554 permits renormalization for estimation of cellular mRNA levels. *J Bacteriol, 183*(16), 4747-
555 4751. doi:10.1128/JB.183.16.4747-4751.2001
556 Hazeltine, W. A., & Block, R. (1973). Synthesis of guanosine tetra- and pentaphosphate requires the
557 presence of a codon-specific, uncharged transfer ribonucleic acid in the acceptor site of
558 ribosomes. *Proc. Natl. Acad. Sci. USA, 70*, 1564-1568.
559 Ingraham, J. L., Maaløe, O., & Neidhardt, F. C. (1983). *Growth of the bacterial cell*: Sinauer
560 Associates, Inc.

561 Jacobson, A., & Gillespie, D. (1968a). Metabolic Events Occurring During Recovery from Prolonged
562 Glucose Starvation in Escherichia coli. *Journal of Bacteriology, 95*(3), 1030. Retrieved from
563 http://jb.asm.org/content/95/3/1030.abstract
564 Jacobson, A., & Gillespie, D. (1968b). Metabolic events occurring during recovery from prolonged
565 glucose starvation in Escherichia coli. *J Bacteriol, 95*(3), 1030-1039. Retrieved from
566 http://www.ncbi.nlm.nih.gov/pubmed/4868350
567 Jain, C. (2018). Role of ribosome assembly in Escherichia coli ribosomal RNA degradation. *Nucleic*
568 *Acids Research, 46*(20), 11048-11060. doi:10.1093/nar/gky808
569 Jinks-Robertson, S., Gourse, R. L., & Nomura, N. (1983). Expression of rRNA and tRNA genes in
570 *Escherichia coli*: Evidence for feedback regulation by products of rRNA operons. *Cell, 33*, 865-
571 876.
572 Kaplan, R., & Apirion, D. (1974). The Involvement of Ribonuclease I, Ribonuclease II, and
573 Polynucleotide Phosphorylase in the Degradation of Stable Ribonucleic Acid during Carbon
574 Starvation in Escherichia coli. *249*(1), 149-151. Retrieved from
575 http://www.jbc.org/content/249/1/149.abstract
576 Kaplan, R., & Apirion, D. (1975). The fate of ribosomes in Escherichia coli cells starved for a carbon
577 source. *J Biol Chem, 250*(5), 1854-1863. Retrieved from
578 https://www.ncbi.nlm.nih.gov/pubmed/1089666
579 Keener, J., & Nomura, K. (1996). *Regulation of ribosome synthesis* (F. C. Neidhardt, R. Curtiss III, J. L.
580 Ingraham, E. C. C. Lin, K. B. Low, B. Magasanik, W. S. Reznikoff, M. Riley, M. Schaechter, & H.
581 E. Umbarger Eds. 2nd ed. ed.). Washington, D.C.: ASM Press.
582 Kjeldgaard, N. O., Maaloe, O., & Schaechter, M. (1958). The Transition between Different
583 Physiological States during Balanced Growth of Salmonella-Typhimurium. *Journal of General*
584 *Microbiology, 19*(3), 607-616. Retrieved from <Go to ISI>://WOS:A1958WM15500019
585 Laffler, T., & Gallant, J. (1974). spoT, a new genetic locus involved in the stringent response in E. coli.
586 *Cell, 1*(1), 27-30. doi:https://doi.org/10.1016/0092-8674(74)90151-2
587 Lazzarini, R. A., Cashel, M., & Gallant, J. (1971). On the regulation of guanosine tetraphosphate levels
588 in stringent and relaxed strains of *Escherichia coli*. *J. Biol. Chem., 246*, 4381-4385.
589 Leavitt, R. I., & Umbarger, H. E. (1961). Isoleucine and valine metabolism in Escherichia coli. X. The
590 enzymatic formation of acetohydroxybutyrate. *J Biol Chem, 236*, 2486-2491. Retrieved from
591 http://www.ncbi.nlm.nih.gov/pubmed/13759955
592 Leavitt, R. I., & Umbarger, H. E. (1962). Isoleucine and valine metabolism in Escherichia coli. XI.
593 Valine Inhibition of the Growth of Escherichia coli Strain K-12. *Journal of Bacteriology, 83*(3),
594 624-630. Retrieved from http://www.ncbi.nlm.nih.gov/pmc/articles/PMC279321/
595 Li, S. H.-J., Li, Z., Park, J. O., King, C. G., Rabinowitz, J. D., Wingreen, N. S., & Gitai, Z. (2018).
596 Escherichia coli translation strategies differ across carbon, nitrogen and phosphorus
597 limitation conditions. *Nature Microbiology, 3*(8), 939-947. doi:10.1038/s41564-018-0199-2
598 Liang, S. T., Xu, Y. C., Dennis, P., & Bremer, H. (2000). mRNA composition and control of bacterial
599 gene expression. *J Bacteriol, 182*(11), 3037-3044. Retrieved from
600 https://www.ncbi.nlm.nih.gov/pubmed/10809680
601 Maaløe, O. (1966). Control of macromolecular synthesis; a study of DNA, RNA, and protein synthesis
602 in bacteria. In N. O. Kjeldgaard (Ed.). New York: W. A. Benjamin.
603 Maaløe, O. (1979). Regulation of the Protein Synthesizing Machinery- Ribosomes, tRNA, Factors,
604 and So On. In R. F. Goldberger (Ed.), *Biological Regulation and Development* (Vol. 1, pp. 487-
605 542). New York: Plenum Press.

606 Maciag-Dorszynska, M., Szalewska-Palasz, A., & Wegrzyn, G. (2013). Different effects of ppGpp on
607 Escherichia coli DNA replication in vivo and in vitro. *FEBS Open Bio, 3*, 161-164.
608 doi:10.1016/j.fob.2013.03.001
609 Mandelstam, J., & Halvorson, H. (1960). Turnover of protein and nucleic acid in soluble and
610 ribosome fractions of non-growing Escherichia coli. *Biochim Biophys Acta, 40*, 43-49.
611 Retrieved from https://www.ncbi.nlm.nih.gov/pubmed/24546427
612 Maruyama, H., & Mizuno, D. (1970). Ribosome degradation and the degradation products in starved
613 Escherichia coli. I. Comparison of the degradation rate and of the nucleotide pool between
614 Escherichia coli B and Q-13 strains in phosphate deficiency. *Biochim Biophys Acta, 199*(1),
615 159-165. Retrieved from http://www.ncbi.nlm.nih.gov/pubmed/4905130
616 Neidhardt, F. C. (1964). The Regulation of RNA Synthesis in Bacteria. In J. N. Davidson & W. E. Cohn
617 (Eds.), *Progress in Nucleic Acid Research and Molecular Biology* (Vol. 3, pp. 145-181):
618 Academic Press.
619 Okamura, S., Maruyama, H. B., & Yanagita, T. (1973). Ribosome Degradation and Degradation
620 Products in Starved Escherichia coli. VI. Prolonged Culture during Glucose Starvation. *The*
621 *Journal of Biochemistry, 73*(5), 915-922.
622 Pato, M. L., & Von Meyenburg, K. (1970). Residual Rna Synthesis in Escherichia-Coli after Inhibition
623 of Initiation of Transcription by Rifampicin. *Cold Spring Harbor Symposia on Quantitative*
624 *Biology, 35*, 497-&. doi:Doi 10.1101/Sqb.1970.035.01.065
625 Paul, B. J., Ross, W., Gaal, T., & Gourse, R. L. (2004). rRNA transcription in Escherichia coli. *Annu Rev*
626 *Genet, 38*(1), 749-770. doi:10.1146/annurev.genet.38.072902.091347
627 Pedersen, S., Reeh, S., & Friesen, J. D. (1978). Functional mRNA half lives in E. coli. *Mol Gen Genet,*
628 *166*(3), 329-336. Retrieved from https://www.ncbi.nlm.nih.gov/pubmed/368581
629 Piir, K., Paier, A., Liiv, A., Tenson, T., & Maivali, U. (2011). Ribosome degradation in growing bacteria.
630 *EMBO Rep, 12*(5), 458-462. doi:10.1038/embor.2011.47
631 Pontes, Mauricio H., Yeom, J., & Groisman, Eduardo A. (2016). Reducing Ribosome Biosynthesis
632 Promotes Translation during Low Mg2+ Stress. *Molecular cell, 64*(3), 480-492.
633 doi:https://doi.org/10.1016/j.molcel.2016.05.008
634 Potrykus, K., Murphy, H., Philippe, N., & Cashel, M. (2011). ppGpp is the major source of growth rate
635 control in E. coli. *Environ Microbiol, 13*(3), 563-575. doi:10.1111/j.1462-2920.2010.02357.x
636 Rao, N. N., Liu, S., & Kornberg, A. (1998). Inorganic Polyphosphate in Escherichia
637 coli: the Phosphate Regulon and the Stringent Response. *Journal of*
638 *Bacteriology, 180*(8), 2186. Retrieved from http://jb.asm.org/content/180/8/2186.abstract
639 Rinas, U., Hellmuth, K., Kang, R., Seeger, A., & Schlieker, H. (1995). Entry of Escherichia coli into
640 stationary phase is indicated by endogenous and exogenous accumulation of nucleobases.
641 *Applied and Environmental Microbiology, 61*(12), 4147-4151. Retrieved from
642 http://www.ncbi.nlm.nih.gov/pmc/articles/PMC167726/
643 Ross, W., Sanchez-Vazquez, P., Chen, A. Y., Lee, J.-H., Burgos, H. L., & Gourse, R. L. (2016). ppGpp
644 binding to a site at the RNAP-DksA interface accounts for its dramatic effects on transcription
645 initiation during the stringent response. *Molecular cell, 62*(6), 811-823.
646 doi:10.1016/j.molcel.2016.04.029
647 Sarmientos, P., & Cashel, M. (1983). Carbon starvation and growth rate-dependent regulation of the
648 Escherichia coli ribosomal RNA promoters: differential control of dual promoters. *Proc Natl*
649 *Acad Sci U S A, 80*(22), 7010-7013. doi:10.1073/pnas.80.22.7010

Schaechter, M., Maaloe, O., & Kjeldgaard, N. O. (1958). Dependency on Medium and Temperature of Cell Size and Chemical Composition during Balanced Growth of Salmonella-Typhimurium. *Journal of General Microbiology, 19*(3), 592-606. Retrieved from <Go to ISI>://WOS:A1958WM15500018

Schreiber, G., Ron, E. Z., & Glaser, G. (1995). ppGpp-mediated regulation of DNA replication and cell division in Escherichia coli. *Curr Microbiol, 30*(1), 27-32.

Sorensen, M. A., Fehler, A. O., & Lo Svenningsen, S. (2018). Transfer RNA instability as a stress response in Escherichia coli: Rapid dynamics of the tRNA pool as a function of demand. *RNA Biol, 15*(4-5), 586-593. doi:10.1080/15476286.2017.1391440

Sørensen, M. A., Kurland, C. G., & Pedersen, S. (1989). Codon usage determines the translation rate in *Escherichia coli*. *J. Mol. Biol., 207*, 365-377.

Spira, B., Silberstein, N., & Yagil, E. (1995). Guanosine 3',5'-bispyrophosphate (ppGpp) synthesis in cells of Escherichia coli starved for Pi. *J Bacteriol, 177*(14), 4053-4058. doi:10.1128/jb.177.14.4053-4058.1995

St John, A. C., & Goldberg, A. L. (1980). Effects of starvation for potassium and other inorganic ions on protein degradation and ribonucleic acid synthesis in Escherichia coli. *Journal of Bacteriology, 143*(3), 1223. Retrieved from http://jb.asm.org/content/143/3/1223.abstract

Stenum, T. S., Sorensen, M. A., & Svenningsen, S. L. (2017). Quantification of the Abundance and Charging Levels of Transfer RNAs in Escherichia coli. *J Vis Exp*(126). doi:10.3791/56212

Sulthana, S., Basturea, G. N., & Deutscher, M. P. (2016). Elucidation of pathways of ribosomal RNA degradation: an essential role for RNase E. *RNA, 22*(8), 1163-1171. doi:10.1261/rna.056275.116

Svenningsen, S. L., Kongstad, M., Stenum, T. S., Munoz-Gomez, A. J., & Sorensen, M. A. (2017). Transfer RNA is highly unstable during early amino acid starvation in Escherichia coli. *Nucleic Acids Res, 45*(2), 793-804. doi:10.1093/nar/gkw1169

Temple, R. J., Umbarger, H. E., & Magasanik, B. (1965). The Effect of L-Valine on Enzyme Synthesis in Escherichia Coli K-12. *J Biol Chem, 240*, 1219-1224. Retrieved from https://www.ncbi.nlm.nih.gov/pubmed/14284728

Traxler, M. F., Summers, S. M., Nguyen, H. T., Zacharia, V. M., Hightower, G. A., Smith, J. T., & Conway, T. (2008). The global, ppGpp-mediated stringent response to amino acid starvation in Escherichia coli. *Mol Microbiol, 68*(5), 1128-1148. doi:10.1111/j.1365-2958.2008.06229.x

Winther, K. S., Roghanian, M., & Gerdes, K. (2018). Activation of the Stringent Response by Loading of RelA-tRNA Complexes at the Ribosomal A-Site. *Molecular cell, 70*(1), 95-+. doi:10.1016/j.molcel.2018.02.033

Zundel, M. A., Basturea, G. N., & Deutscher, M. P. (2009). Initiation of ribosome degradation during starvation in Escherichia coli. *RNA, 15*(5), 977-983. doi:10.1261/rna.1381309

Data Availability

The data that support the findings of this study are available from the corresponding author upon reasonable request.

Figure Legends

Figure 1. Growth parameters for a culture starved for isoleucine by addition of valine. A culture in balanced growth received 400 µg/ml valine to induce starvation at time zero (vertical line at time 0) and additionally 100 µg/ml extra valine every hour. After 8 hours the culture received 400 µg/ml of isoleucine to end the starvation (vertical line at 8h).
Optical density at 436 nm (A), accumulation of radioactivity in protein (B), accumulation of radioactivity in RNA (C) and accumulation of radioactivity in DNA (D) were measured during 80 minutes of exponential growth and 8 hours of isoleucine starvation in a pyrimidine- and arginine-auxotroph *E. coli* strain. CFU (colony forming units) were measured for 8 hours of starvation (E). All y-axes are $\log_{10}$ transformed.

Figure 2. Northern blot showing degradation kinetics for rRNA during valine-induced isoleucine limitation. A: A 1 % agarose gel was used for electrophoresis of total RNA from samples harvested immediately before starvation (lanes 1-3), during starvation at the indicated times (lanes 4-8), after starvation was ended by addition of isoleucine (lanes 9-13) and from spike-in cells only (lane 14) and was blotted. The resulting membrane was probed for $tRNA^{Sec}$ and 5S, 16S and 23S rRNA as indicated on the left. **B:** The levels of 5S, 16S and 23S rRNAs were quantified by normalizing to $tRNA^{SelC}$ originating from the spike-in cells (Svenningsen et al., 2017). Spike-in-normalized RNA levels are shown relative to the average of the three RNA samples harvested prior to starvation. Error bars indicate SEM (n=3). **C:** Growth of the culture before, during and after starvation.

Figure 3. Quantification of rRNA reduction during starvation. A: Glucose starvation (n=5) **B:** phosphate starvation (n=3) **C:** rifampicin treatment (n=3). **D:** Growth curves for cultures starved for glucose, phosphate or treated with 100 µg/ml of rifampicin. Vertical line indicates time of filtration and resuspension in starvation medium (red or blue curve), or rifampicin treatment (orange curve). To ease evaluation of the growth curves, all OD measurements obtained after filtration were corrected for the loss of of cells (10-20%) that occurred during filtration into glucose-free or phosphate-free medium. It was assumed that there is no change in OD after rifampicin treatment. Samples were harvested and treated as in Fig. 2.

Figure 4. Detection of 16S rRNA levels with FISH during glucose starvation (n=3), isoleucine starvation (n=3), phosphate starvation (n=3), and 80 min. of rifampicin treatment (n=3). Cells were fixed prior to or after 80 minutes of starvation. A probe complementary to a sequence in the 16S rRNA (1482-1499) was allowed to hybridize overnight. The fluorescent signal was measured by flow cytometry. In addition, starved (n=2) and unstarved (n=2) cells were fixed and incubated overnight with RNase A, before the florescent probe was added. Representative scatter plots from exponential phase cells (A) and isoleucine starved cells (B) are shown. 16S rRNA levels were quantified (C). To test for significance a t-test was applied (* = p-value < 0.05, ** = p-value < 0.01) Normal distribution was assumed for samples only repeated two times. Error bars indicate SEM. a.u. = arbitrary unit.

Figure 5. *In vivo* assay of RNA degradation products during isoleucine starvation, glucose starvation, phosphate starvation and rifampicin treatment. Wildtype MAS1081 cells

incorporated [^{14}C]-uracil for 5 generations before filtration and resuspension in media inducing starvation or containing rifampicin. Samples were taken every 30 minutes until refeeding, at which point sampling was briefly intensified. The vertical line indicates when the three starved cultures were replenished with the missing nutrient (glucose, isoleucine or phosphate). Degradation was determined by plotting the formic-acid-soluble radioactivity as a percentage of the sum of radioactivity from the formic-acid-soluble and TCA-precipitable fractions, from three independent experiments. Error bars indicate SEM (n=3).

Figure 6: Data on 16S rRNA levels from Fig. 2 and 3 plotted in the same graph to ease comparison between the different treatments.

Figure 7. Major regulatory pathways for the homeostasis of translational RNA components as a function of nutrient influx. Blue connectors indicate pathways dominant during growth while red connectors indicate pathways active upon a downshift in nutrient availability. Arrowheads indicate an increase in the component it points to while T-bars represent a decrease. Squared brackets mean "concentration of". Numbers in circles indicate the following representative references. 1: (Maaløe, 1979) 2: (Bremer & Dennis, 2008) 3: (Svenningsen et al., 2017) ; 4:(Cashel & Gallant, 1969; Ross et al., 2016) 5: (Gausing, 1977; Jain, 2018) 6: (Zundel et al., 2009) and present data 7: (Hazeltine & Block, 1973; Winther et al., 2018) 8: (Sørensen et al., 1989; Dong et al., 1996).

Figure 1

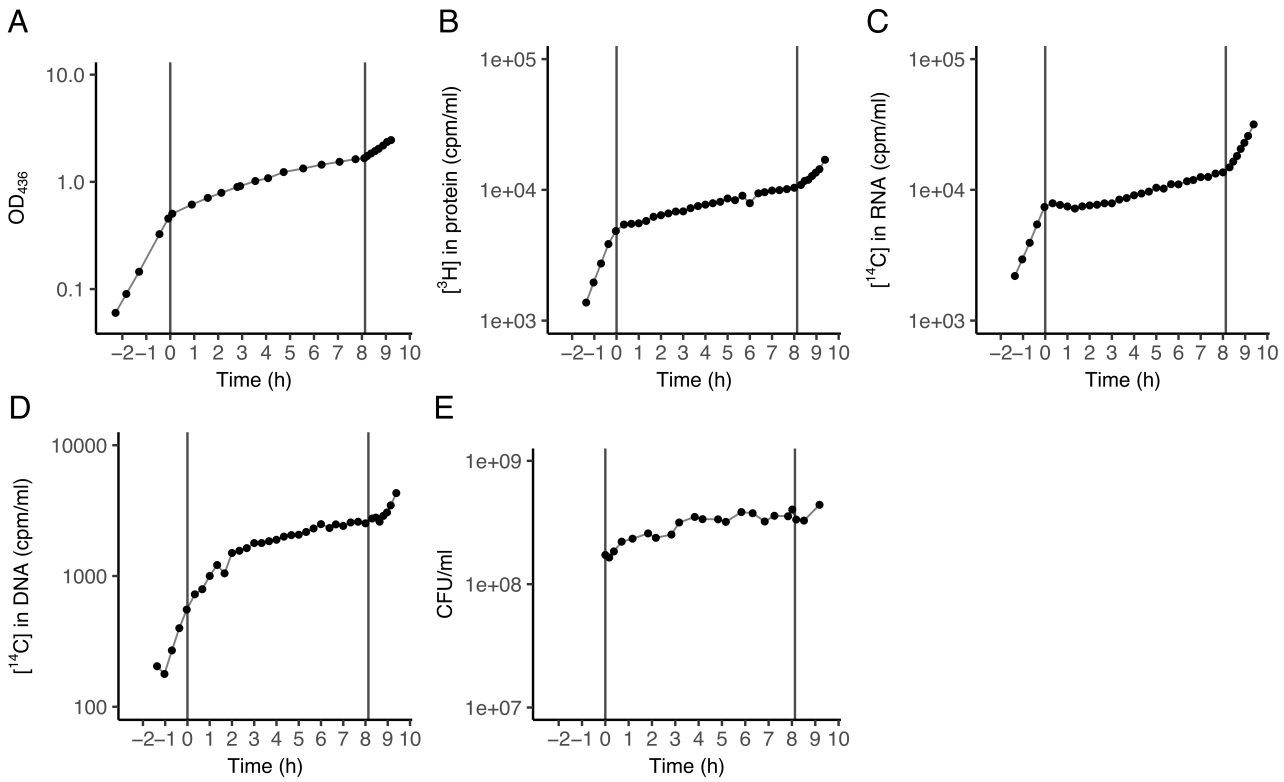
A
B
C
D
E
OD436
[3H] in protein (cpm/ml)
[14C] in RNA (cpm/ml)
[14C] in DNA (cpm/ml)
CFU/ml
Time (h)
10.0
1.0
0.1
1e+05
1e+04
1e+03
10000
1000
100
1e+09
1e+08
1e+07
−2 −1 0 1 2 3 4 5 6 7 8 9 10

Figure 2

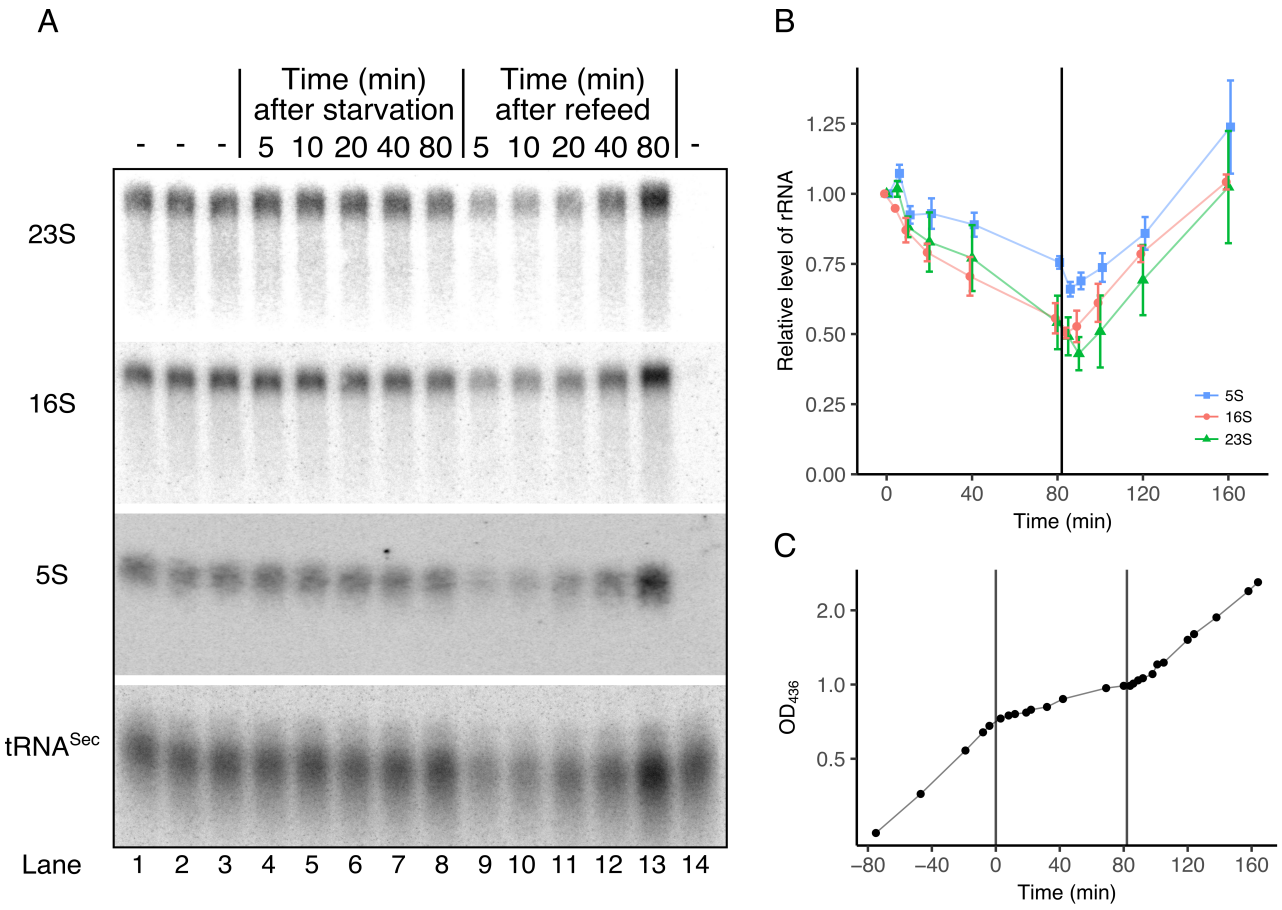
A
Time (min) after starvation
Time (min) after refeed
- - - 5 10 20 40 80 5 10 20 40 80 -
23S
16S
5S
tRNASec
Lane 1 2 3 4 5 6 7 8 9 10 11 12 13 14
B
Relative level of rRNA
1.25
1.00
0.75
0.50
0.25
0.00
0 40 80 120 160
Time (min)
5S
16S
23S
C
OD436
2.0
1.0
0.5
−80 −40 0 40 80 120 160
Time (min)

Figure 3

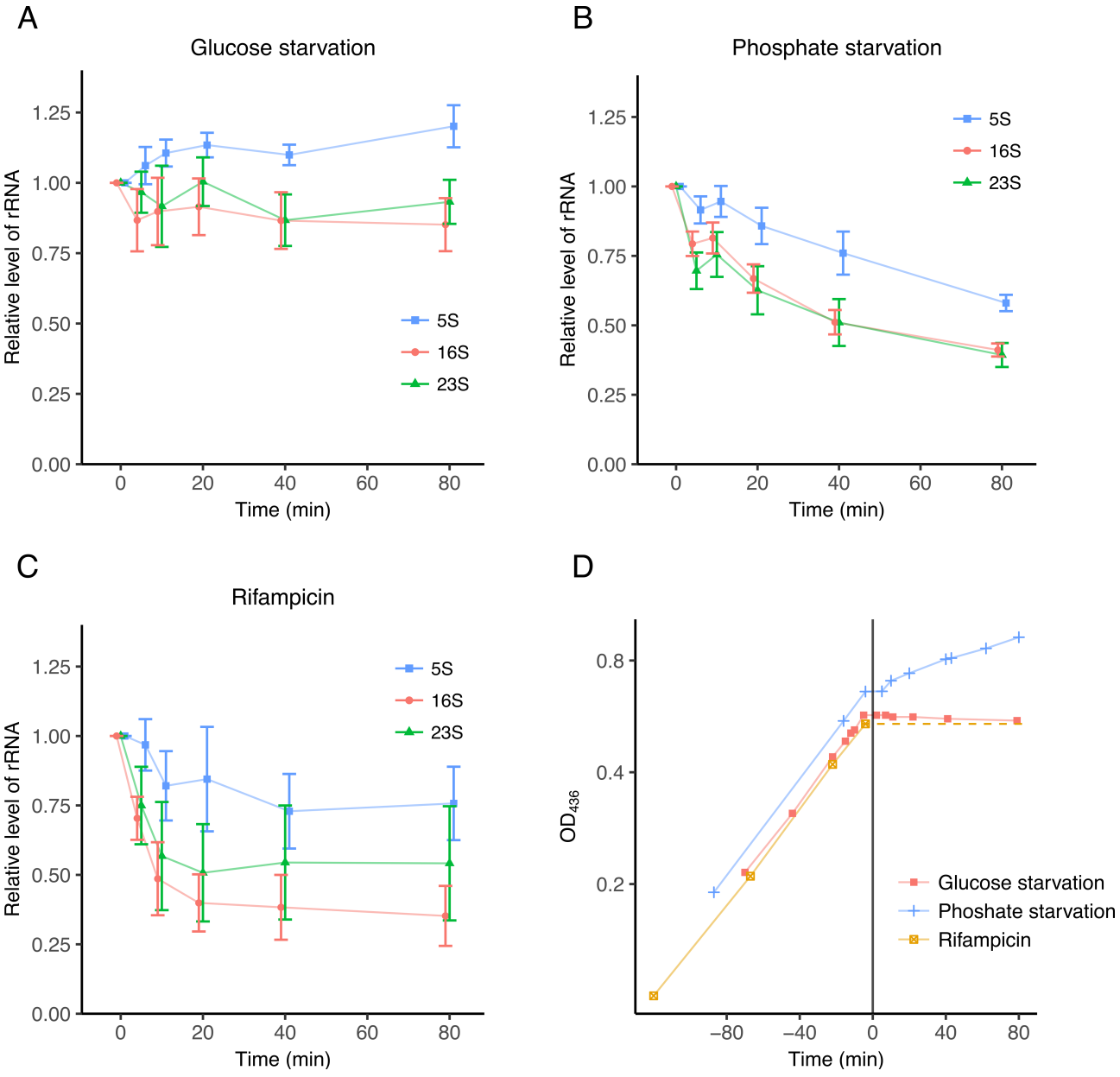
A
Glucose starvation
Relative level of rRNA
1.25
1.00
0.75
0.50
0.25
0.00
0
20
40
60
80
Time (min)
5S
16S
23S
B
Phosphate starvation
Relative level of rRNA
Time (min)
5S
16S
23S
C
Rifampicin
Relative level of rRNA
Time (min)
5S
16S
23S
D
OD436
0.8
0.4
0.2
−80
−40
0
40
80
Time (min)
Glucose starvation
Phoshate starvation
Rifampicin

Figure 4

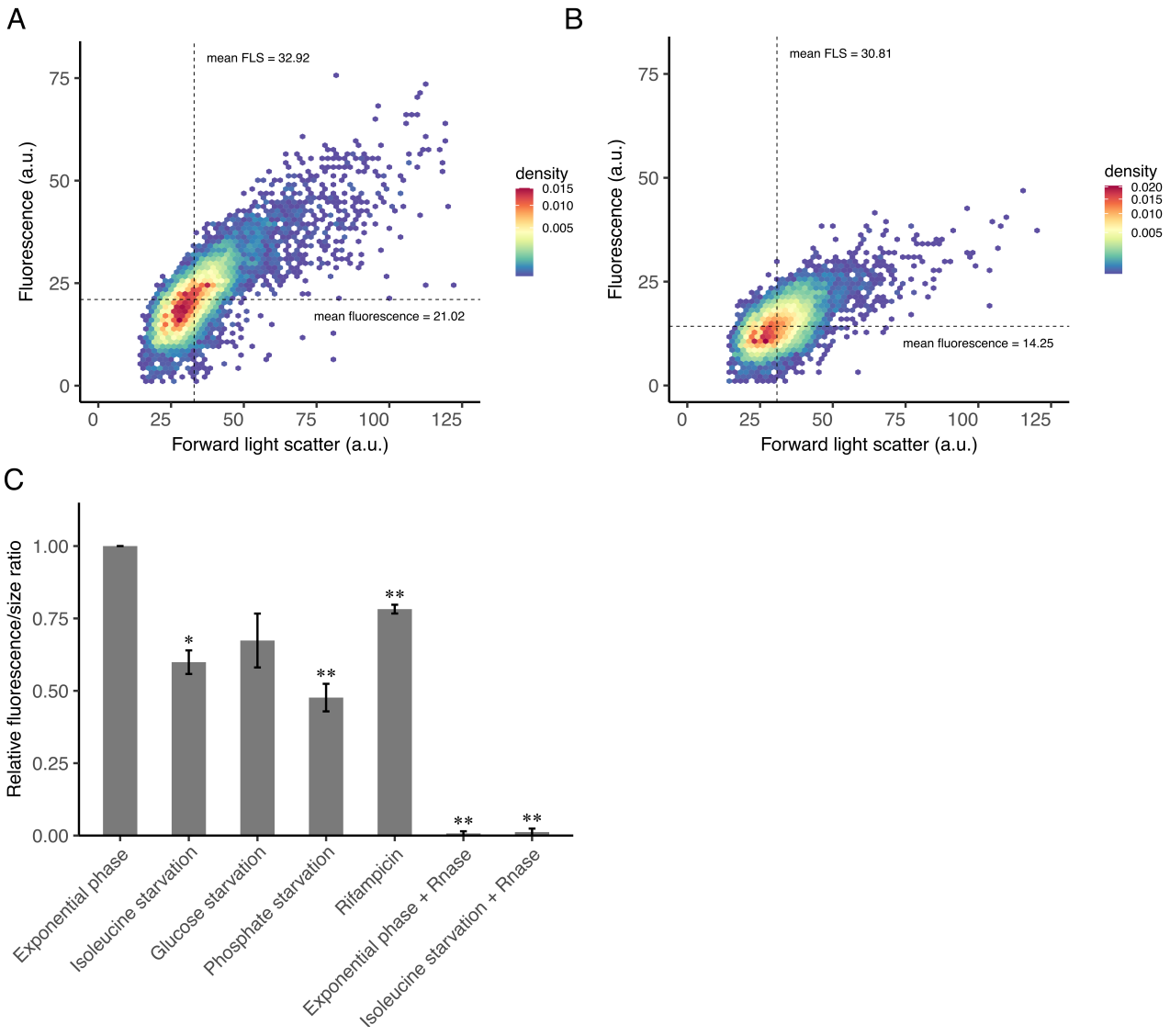
A
mean FLS = 32.92
mean fluorescence = 21.02
Fluorescence (a.u.)
Forward light scatter (a.u.)
density
0.015
0.010
0.005
B
mean FLS = 30.81
mean fluorescence = 14.25
Fluorescence (a.u.)
Forward light scatter (a.u.)
density
0.020
0.015
0.010
0.005
C
Relative fluorescence/size ratio
1.00
0.75
0.50
0.25
0.00
*
**
**
**
**
Exponential phase
Isoleucine starvation
Glucose starvation
Phosphate starvation
Rifampicin
Exponential phase + Rnase
Isoleucine starvation + Rnase

Figure 5

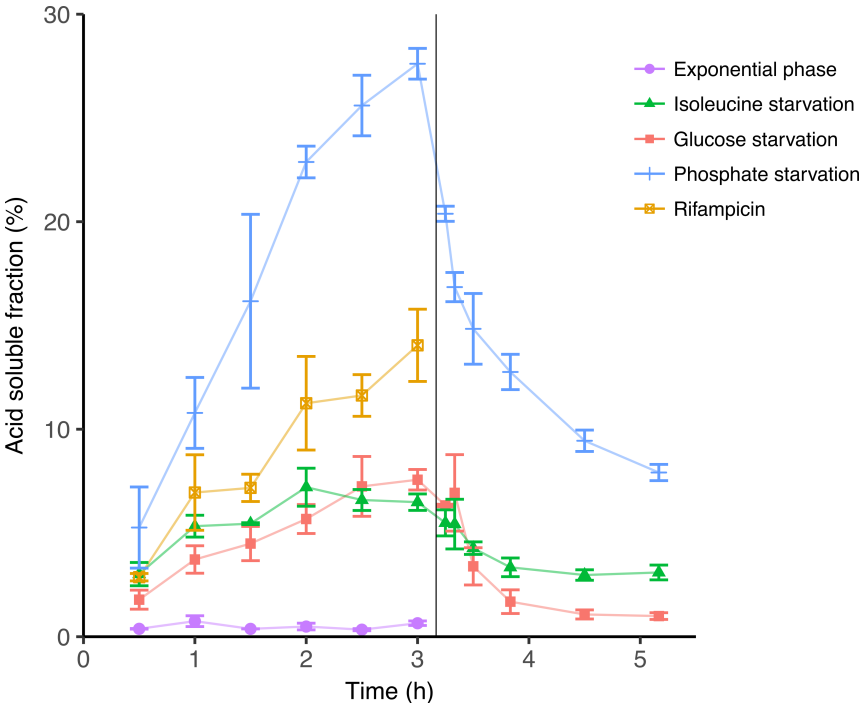
Acid soluble fraction (%)
30
20
10
0
0
1
2
3
4
5
Time (h)
Exponential phase
Isoleucine starvation
Glucose starvation
Phosphate starvation
Rifampicin

Figure 6

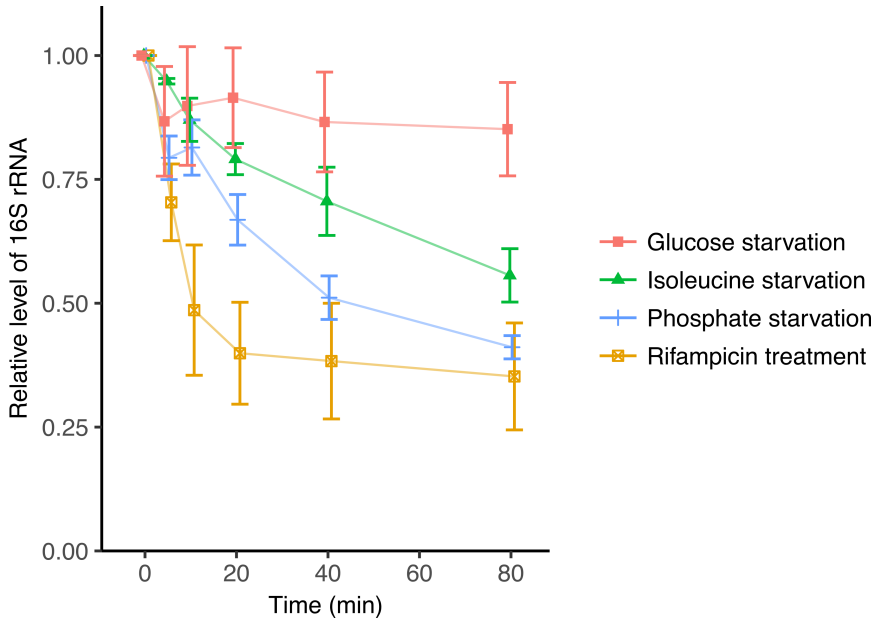
Relative level of 16S rRNA
1.00
0.75
0.50
0.25
0.00
0
20
40
60
80
Time (min)
Glucose starvation
Isoleucine starvation
Phosphate starvation
Rifampicin treatment

Figure 7

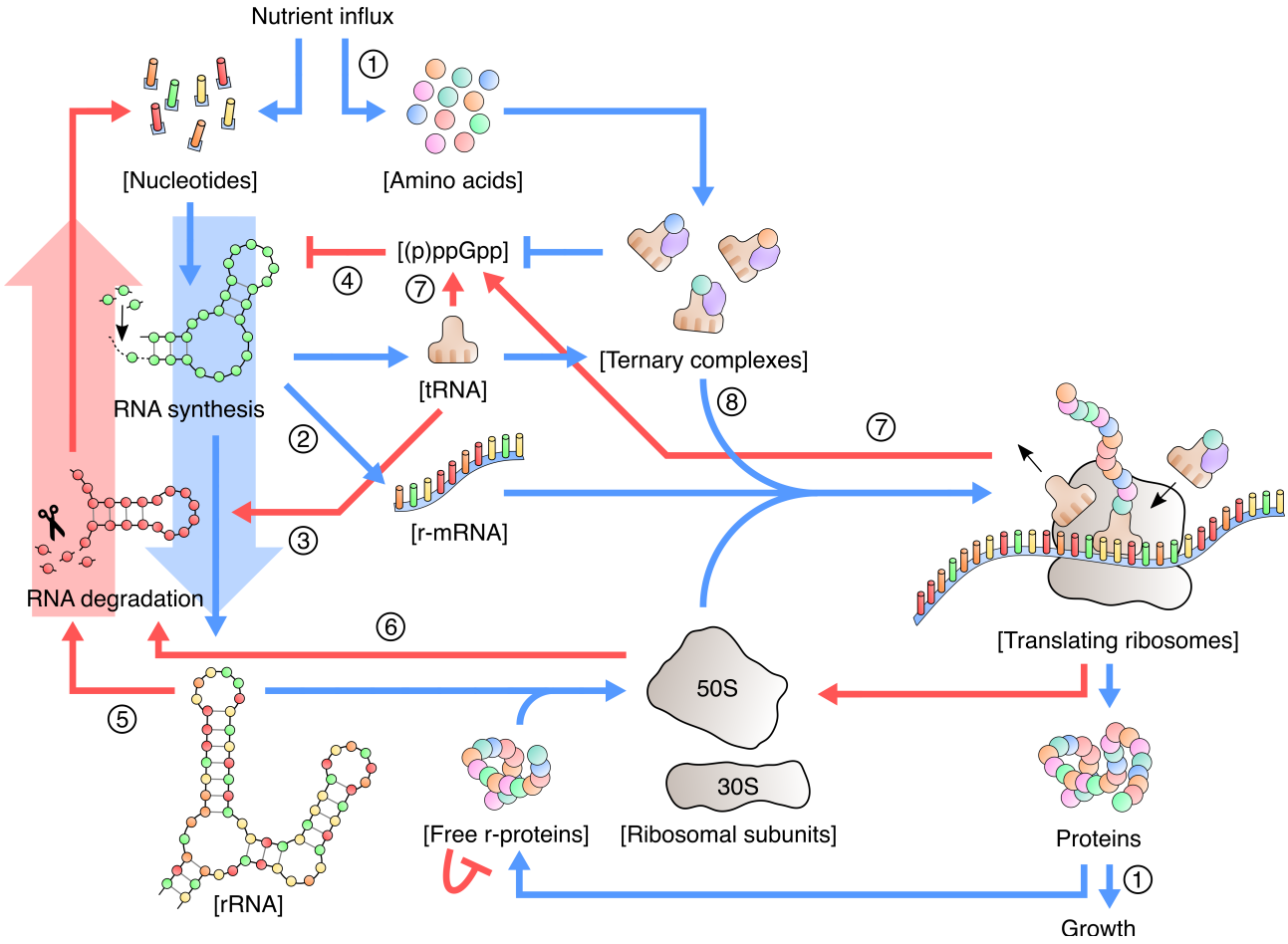
Nutrient influx
①
[Nucleotides]
[Amino acids]
[(p)ppGpp]
④
⑦
[Ternary complexes]
RNA synthesis
[tRNA]
⑧
⑦
②
[r-mRNA]
③
RNA degradation
⑥
[Translating ribosomes]
50S
⑤
30S
[Free r-proteins]
[Ribosomal subunits]
Proteins
①
[rRNA]
Growth

Supplementary Discussion

Optical density as a reference for normalization

The question of how to best relate RNA quantities to the amount or mass of cells in the culture at the time of RNA harvest is not trivial. In the figures in the main text we normalized RNA levels to the optical density of the culture by adjusting the volume of spike-in cells added to each sample according to the OD_{436} of the sampled culture. However, we would like to draw attention to the point that while the change in optical density provides a clear measure of the growth of a bacterial culture in steady-state, since all constituents grow with the same rate, changes in optical density are complex to interpret upon disruption of the steady-state. This is because the light scatter measured as optical density does not directly report on one physical parameter of the culture. OD is most closely related to the dry weight of the cells but is also affected by alterations in cell size, cell shape, and macromolecular content [1]. Thus, for example, storage of carbon as glycogen could account for the rise of OD in a phosphate- or nitrogen-starved culture [2]. As shown in Supplementary Figure S2, the three types of starvation employed in this study caused dramatically decreased growth rates as measured by OD as expected, but the OD profiles of the starved cultures varied somewhat between the three conditions (Fig. S2A). The OD of isoleucine-starved cultures continued to rise after the addition of valine, while the OD of glucose-starved cultures did not, and phosphate-starved cultures showed an intermediate phenotype. To provide a more complete characterization of rRNA levels after the four treatments, Figure 6 (main text) shows the levels of 16S rRNA measured under the four conditions normalized to OD_{436}, while Figure S2B shows the same rRNA measurements normalized only to the culture volume, thereby disregarding effects of the differences in OD profiles. Figure S2B illustrates clearly that the different types of starvation lead to different

kinetics of rRNA decrease in the cultures irrespective of their OD profiles. Since the OD of the glucose-starved culture did not change during the starvation period, and the OD of the rifampicin-treated culture was assumed to remain unchanged, these two graphs appear identical in Fig. 6 and S2B. For the isoleucine-starved and phosphate-starved cultures, the net results of 16S rRNA transcription and degradation are 20% and 40% drops in 16S rRNA per culture volume after 80 min, respectively (Fig. S2B). In conclusion, the rRNA is unstable but the calculation of the rate of degradation is not independent on which cellular component it is related to.

References to Supplementary discussion:

1. Koch, A.L., *Turbidity measurements of bacterial cultures in some available commercial instruments.* Anal Biochem, 1970. **38**(1): p. 252-9.
2. Dietzler, D.N., M.P. Leckie, and C.J. Lais, *Rates of glycogen synthesis and the cellular levels of ATP and FDP during exponential growth and the nitrogen-limited stationary phase of Escherichia coli W4597 (K).* Arch Biochem Biophys, 1973. **156**(2): p. 684-93.

Supplementary Materials and Methods

Detailed Materials and Methods.

Northern blots

After hot phenol extraction the RNA was ultimately resuspended in 50µl 10 mM NaOAc (pH 4.7), 1 mM EDTA and stored until use at -80°C.

Electrophoresis through a 1% MOPS buffered agarose gel prepared with 6% formaldehyde was used for RNA separation. 5µl sample was loaded in 15 µl loading dye (0.1 M NaOAc, 8 M urea, bromophenol blue). RNA was blotted on to a Hybond-N+ membrane under pressure (capillary blot) overnight and crosslinked to the membrane by 0.12 J/cm^2 of UV light in a UVC 500 UV crosslinker. Membranes were pre-hybridized for one hour at 42°C in 6 ml hybridization solution (0.09 M NaCl, 0.05 M NaH_2PO_4 (pH 7.7), 5 mM EDTA, 5x Denhardt's solution, 0.5% (w/v) SDS, 100 mg/ml sheared, denatured herring sperm DNA) before adding the radioactive probe for overnight hybridization. Probes (sequences in Table S1) were made by polynucleotide kinase mediated labeling of DNA-oligos in the 5'-end with γ-[^{32}P]-ATP. Prior to visualization of radioactivity with a phosphorimager scanner the membranes were washed three times in 0.3 M NaCl, 30 mM sodium citrate, 0.1 % SDS. Probes were removed with boiling "stripping" buffer (0.1% SDS, 18 mM NaCl, 1 mM NaH_2PO_4, 0.1 mM EDTA). Removal was monitored with at Geiger-Müller counter and once satisfactory a new probe was used.

Macromolecular synthesis measurements

Samples for total DNA, RNA and protein, was left to precipitate in the 5% TCA solution at 0°C for 1 hour, followed by filtration through a glass fiber filter. In the NaOH solution RNA is hydrolyzed whilst DNA remains intact. The NaOH samples were incubated at 37°C for 2 hours,

acidified with 1 ml 10% TCA and finally filtered like the TCA samples. The filters were dried for 30 minutes at 65°C, 5 ml scintillation fluid was added and radioactivity was measured in a scintillation counter. The amount of radioactivity in RNA was estimated by subtracting the ^{14}C counts found in DNA (NaOH samples) from the ^{14}C counts found in the RNA+DNA samples harvested directly into TCA at the same time point. The CPM_0 value for each substance, representing the radioactivity not incorporated before its addition, was estimated by a differential plot (CPM incorporated as a function of OD_{436}) and the value was added to all measurements before plotting.

Colony forming units (CFU) was measured by a dilution series of 50 µl culture into M63 buffer (15 mM $(NH_4)_2SO_4$, 1.8 µM $FeSO_4$, 1 mM $MgSO_4$, 100 mM KH_2PO4). Once appropriately diluted, 0.5 ml was spread on agar plates and incubated O/N at 37°C. The next day colonies were counted.

Table S1. Probe sequences:

5S rRNA	5'-acactaccatcggcgctac-3'
16S rRNA	5'-aaggaggtgatccaaccgca-3'
16S rRNA FISH	5'-tacgacttcaccccagtc-3'
23S rRNA	5'-tatcagcctgttatccccgg-3'
$tRNA^{Sec}$	5'-atttgaagtccagccgcc-3'

Monitoring of rRNA degradation in vivo

The cells were filtered and immediately resuspended in MOPS with 400 µg/ml valine, MOPS with 0.2 % glucose, MOPS with 100 µg/ml rifampicin or MOPS without glucose or MOPS without phosphate. Samples were harvested every 30 minutes by transferring 0.5 ml culture into 5 ml 0°C 5% TCA and an additional 0.5 ml culture into 0.25 ml 4 M formic acid, also 0°C (Cohen and Kaplan, 1977). The formic acid samples were incubated at 0°C for 15 minutes. After centrifugation at 4°C, 200 µl of the supernatant was transferred to a vial and neutralized with 260

µl 1 M Tris base. The TCA samples were left for precipitation at 0°C overnight followed by filtration through glass fiber filters. Filters were left to dry at 65°C for 30 minutes. 5 ml scintillation fluid was added to all samples. Radioactivity was measured in a scintillation counter. Background from the scintillation fluid and filters was subtracted and the counts in the formic acid was then plotted as a percentage of the total counts (i.e. counts in the formic acid + counts in the TCA treated samples).

Fluorescent in situ hybridization

The cells were sampled by centrifugation. The pellet was resuspended in 1 ml 4% formaldehyde and left for 3 hours at room temperature and these fixed cells were permeabilized and dried with ethanol, resuspended in hybridization solution (20mM Tris-HCl (pH 8), 0.9 M NaCl, 0.01% SDS, 40% formamide) and left to pre-hybridize for 30 minutes at 37°C.

Yilmaz and coworkers [3] designed FISH probes to cover the entire 16S rRNA sequence and the brightness of the fluorescent signal was shown to vary with each probe. Based on this work a probe was designed (16S rRNA FISH, Table S1). This cy3-labeled DNA-oligo was added and left for hybridization overnight, also at 37°C. The fixed cells were washed and resuspended in 0.1x SSC (pH 7.3) before fluorescence was measured.

References to Supplementary Methods:

3. Yilmaz, L.S., H.E. Okten, and D.R. Noguera, *Making all parts of the 16S rRNA of Escherichia coli accessible in situ to single DNA oligonucleotides.* Appl Environ Microbiol, 2006. **72**(1): p. 733-44.

Supplementary figures:

Figure S1

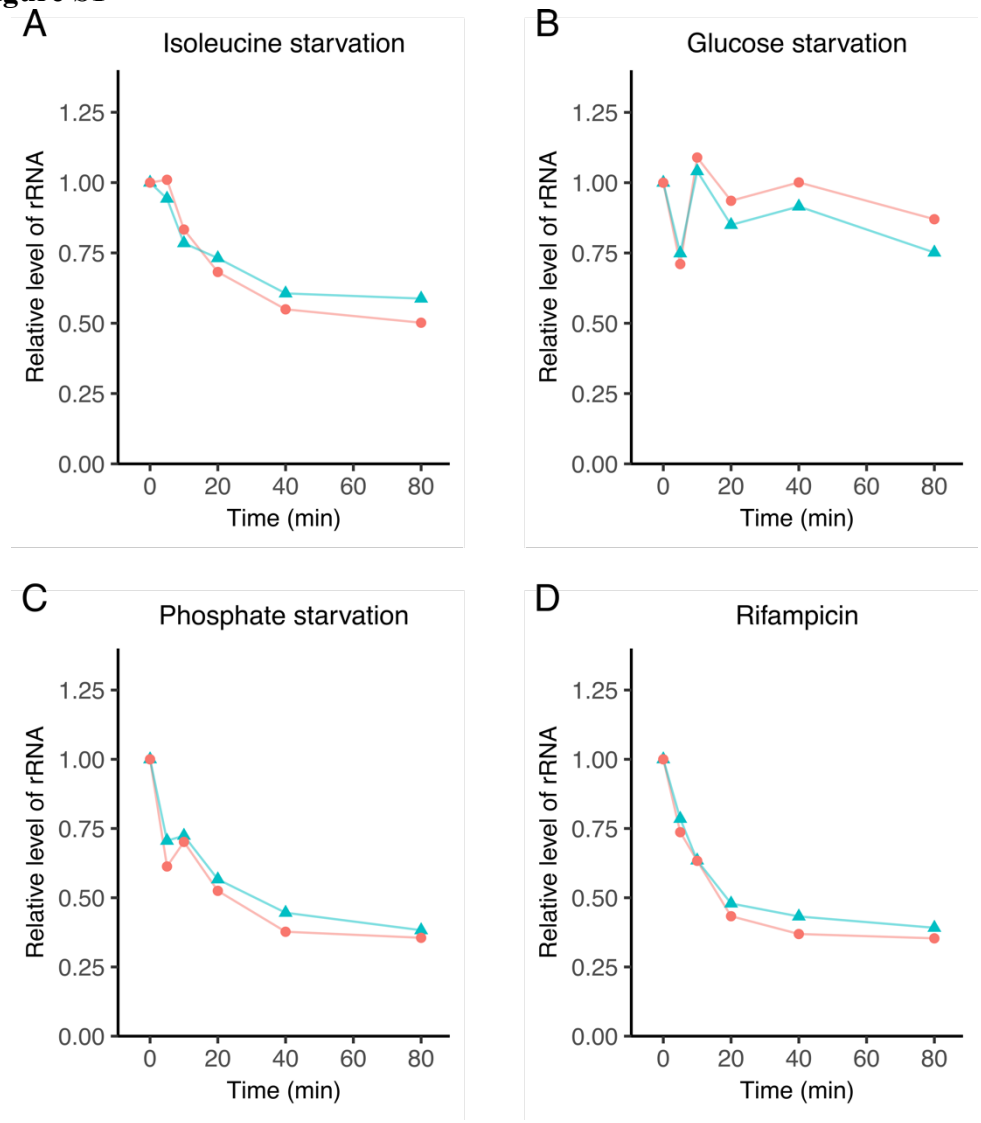

Supplementary Figure S1. Re-probing of Northern blots with FISH probe sequence. Quantification with the same sequence used in the FISH probe of 16S (red points) compared to the quantification obtained with the probe used for the other Northern blot data (blue triangles). A: Ile starvation; B: Glucose starvation; C: Phosphate starvation and D: Rifampicin addition.

Figure S2

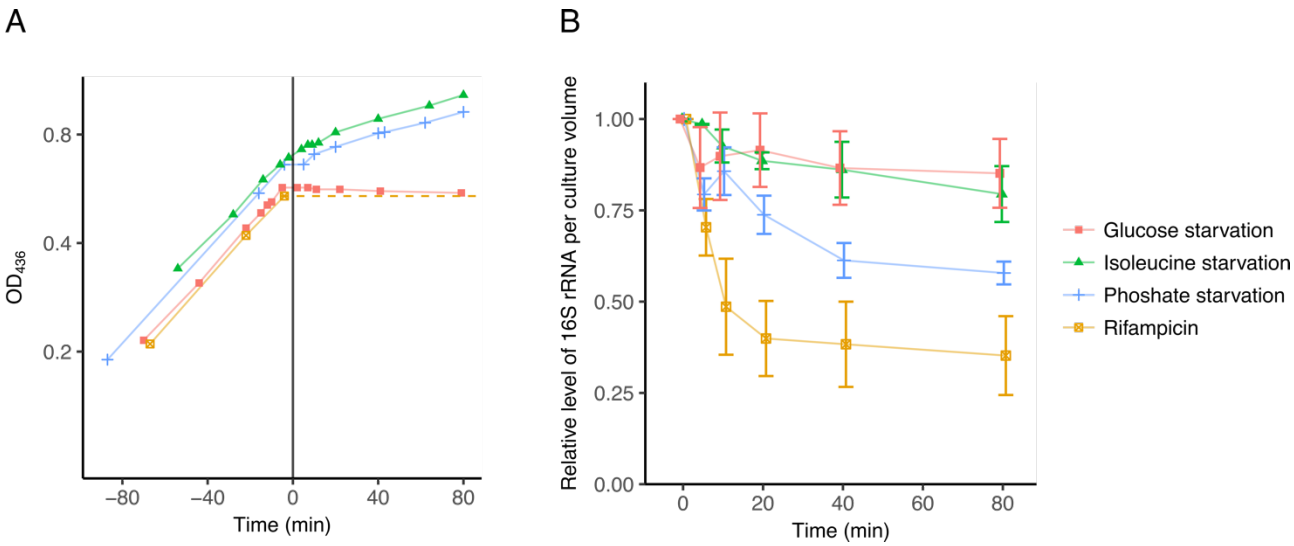

Figure S2: Optical density versus culture volume as a reference point. Data from Figure 6 recalculated without normalization to OD. A: Growth curves for cultures starved for glucose, phosphate or isoleucine from Figs. 2 and 3. B: Summary of 16S rRNA levels from Figs. 2 and 3 calculated per culture volume.